rules for this reaction allow the neutron to carry into the residual nucleus an orbital angular momentum of 0, 2, or 4 units, while the shell model requires that $l_n=2$, corresponding to the addition of a $d_{3/2}$ neutron to the configuration of Cl^{35}.

The experimental data are plotted in Fig. 1 along with the angular distribution of the protons predicted by the Butler[3]

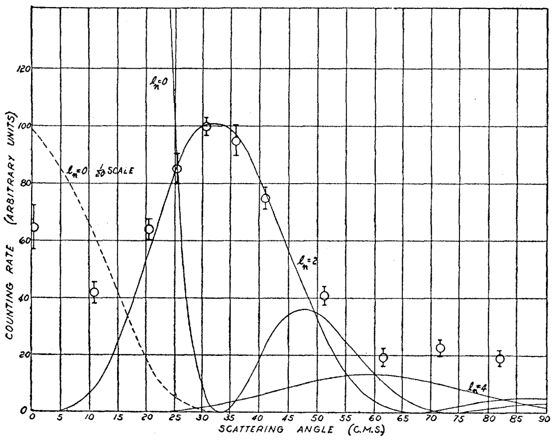

FIG. 1. The angular distribution of the protons associated with the ground state for the reaction $Cl^{35}(d, p)Cl^{36}$. The solid curves are calculated from the Butler theory.

theory for values of $l_n=0$, 2, and 4. The theoretical curves were computed using values of $r_0=5.5\times10^{-13}$ cm, $a=0.23\times10^{13}$ cm^{-1}, and $b=1.4\times10^{13}$ cm^{-1}. The incident deuteron energy was 6.90 Mev (c.m. system) and the Q of the reaction was measured to be 6.3 Mev in good agreement with Shrader and Pollard[4] and with Ennis.[5]

The target, a foil of silver chloride 0.0003 inch thick, was rolled from a pure silver chloride crystal. The background counting rate was obtained by substituting for the silver chloride target a foil of pure silver containing very nearly the same amount of silver per square centimeter as that of the target. It was negligible at all angles except 0°, where it accounted for 35 percent of the total counting rate. In Fig. 1 the vertical lines through the experimental points represent the standard deviations as determined from the

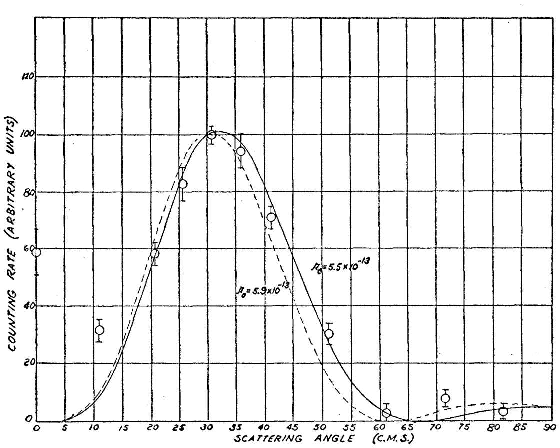

FIG. 2. The angular distribution of Fig. 1 replotted after subtracting from each point the constant "background" counting rate at 65°. The solid curves are calculated from the Butler theory for two values of r_0.

total number of counts and do not represent the over-all uncertainty of the data.

Although (d, p) reactions proceed mainly by means of a stripping process, other processes, such as compound nucleus formation, offer competition. These, however, do not show such marked angular dependence.[6] Because of the competitive processes the measured values do not become zero where indicated by the Butler curves. Since it is difficult to obtain a reliable estimate of the relative cross sections, we subtracted from each point of Fig. 1 an amount equal to the counting rate at 65° and replotted the renormalized data in Fig. 2. The theoretical curves for $l_n=2$ for two values of r_0 are included. Much better agreement is obtained for angles of 20° and larger.

The results of the measurement indicate that the neutron carries mainly two units of orbital angular momentum into the residual nucleus and is presumably a $d_{3/2}$ nucleon as required by the shell model. Assuming that the ground state is a single level (there is some evidence of a doublet structure as in the case of P^{32}), the amount of admixture of $l_n=0$ appears to be less than 4 percent. It is difficult to set a limit on the $l_n=4$ admixture, particularly because of the uncertainty in the "background." It is, however, presumably small.

* This work was supported in part by the AEC and the Michigan Memorial Phoenix Project.
1 H. A. Bethe and S. T. Butler, Phys. Rev. **85**, 1045 (1952).
2 Parkinson, Beach, and King, Phys. Rev. **87**, 387 (1952).
3 S. T. Butler, Proc. Roy. Soc. (London) **A208**, 559 (1951).
4 E. F. Shrader and E. Pollard, Phys. Rev. **59**, 277 (1941).
5 W. W. Ennis, Phys. Rev. **82**, 304 (1951).
6 L. Wolfenstein, Phys. Rev. **82**, 690 (1951).

Nuclear Spin of V^{50} by Paramagnetic Resonance*

C. KIKUCHI,† M. H. SIRVETZ, AND V. W. COHEN
Brookhaven National Laboratory, Upton, New York
(Received August 15, 1952)

WE have investigated the hfs in the paramagnetic resonance absorption spectrum of a Tutton salt of vanadium, enriched to 22.83 percent of V^{50}, and find evidence that the spin of V^{50} is 6. This nucleus, consisting of 23 protons and 27 neutrons, was expected on the basis of Nordheim's rule[1] to have a spin of 7, or near this maximum value. Hitchcock[2] has recently made shell-theoretical calculations based on various potential functions and finds that the state $I=6$ lies lowest for a δ-function potential.

The crystals of $V(NH_4)_2(SO_4)_2\cdot6H_2O$ diluted in the corresponding zinc salt were grown from a solution prepared by using 10 mg of V_2O_5 with a V:Zn ratio of about 1.5:100. A sample of V_2O_5 enriched in V^{50} was supplied by the Stable Isotopes Research and Production division of the AEC. Measurements were performed on several specimens, each approximately 5 mm long and 2 mm in diameter, inserted axially into a cylindrical transmission cavity operating in the TE_{011} mode at approximately 23,000 Mc/sec. The rf was kept constant in frequency while the magnetic field was modulated at 60 cps over a range of approximately 80 gauss.

The observed spectrum consisted of 8 strong lines, corresponding to $I(V^{51})=7/2$,[3] and a number of weak components which have been assigned to V^{50}. The intensity ratio of weak to strong lines was approximately 1:5 and their relative splittings 0.39. The spectrum can be calculated from the known g-values[4,5] and isotopic abundance for various V^{50} spin values. Figure 1 shows the spectrum that is expected for $I(V^{50})=6$ and 7. The calculated relative splitting is 0.38 and the intensity ratio, for $I=6$, is 1:5.5.

In all samples used we observed the components corresponding to $-6\leq m\leq6$, excepting those for $m=\pm4$, which, according to

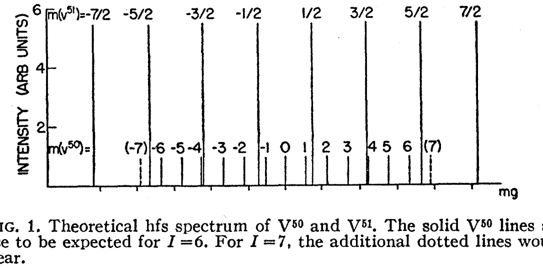

FIG. 1. Theoretical hfs spectrum of V^{50} and V^{51}. The solid V^{50} lines are those to be expected for $I=6$. For $I=7$, the additional dotted lines would appear.

theory, should almost coincide with the strong V^{51} lines. The lines for $m=\pm 7$ were not observed, and considerable effort was directed towards demonstrating that these components would have been observed if present. In Fig. 2(a) we show the lines $m=5/2$ of

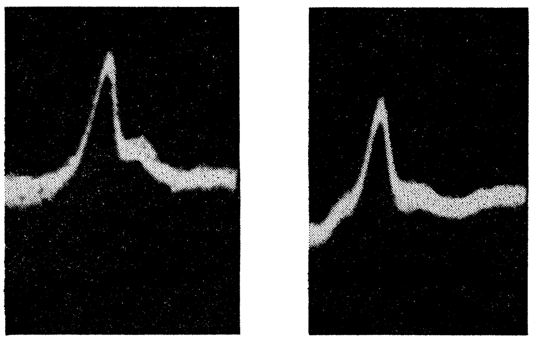

FIG. 2. Photographs of two sections of spectrum. (a) The line $m=-5/2$ of V^{51} and the satellite $m=-6$ of V^{50}; (b) lines $m=1/2$ of V^{51} and $m=1$ and 2 of V^{50}.

V^{51} and $m=-6$ of V^{50} separated by 20 gauss. Figure 2(b) shows that line $m=+1/2$ of V^{51} with the partially resolved lines $m=+1$ and $+2$ of V^{50}, the measured separations from the main peak being 21 and 14 gauss. Therefore, we conclude that the line for $m=-7$ would have been observed if V^{50} spin were 7. No line attributable to $I>7$ was observed.

* Work done at Brookhaven National Laboratory under the auspices of the AEC.
† On leave from Michigan State College.

[1] L. W. Nordheim, Revs. Modern Phys. **23**, 322 (1951).
[2] A. Hitchcock, Phys. Rev. **87**, 664 (1952).
[3] Bleaney, Ingram, and Scovil, Proc. Phys. Soc. (London) **A64**, 601 (1951); C. A. Hutchison, ONR Technical Report (1951) (unpublished).
[4] W. Knight and V. W. Cohen, Phys. Rev. **76**, 1421 (1949); W. G. Proctor and F. C. Yu, Phys. Rev. **81**, 20 (1951).
[5] Walchli, Leyshon, and Scheitlin, Phys. Rev. **85**, 922 (1952).

High Energy Nuclear Reactions and the Goldberger Model*

J. W. MEADOWS
Cyclotron Laboratory, Harvard University, Cambridge, Massachusetts

(Received August 14, 1952)

According to a model first proposed by Serber[1] and developed in greater detail by Goldberger,[2] high energy nuclear reactions are usually considered as occurring in two steps. First, a high energy particle (100 Mev or greater) may pass through a nucleus, perhaps knocking out one or more nucleons and leaving the residual nucleus in an excited state. Second, this excited nucleus may evaporate other nucleons or emit photons according to the statistical theory. If we can determine the probabilities of the various processes in the first step and the distribution of excitation energy in the residual nucleus, it should be possible to apply the statistical theory to calculate reaction cross sections. Estimates for (p, n), $(p, 2n)$, $(p, 2p)$, and (p, pn) reactions for incident protons of 100 Mev have been made in the region of $A=64$.

Reactions of the above types can proceed in one or more of the following ways:

$$\begin{array}{ll} p+A\rightarrow C_1^*+p; & C_1^*\rightarrow B_1+n \\ & C_1^*\rightarrow B_2+p \\ p+A\rightarrow C_2^*+n; & C_2^*\rightarrow B_3+n \\ & C_2^*\rightarrow B_1+p \\ & C_2^*\rightarrow B_4+\gamma \\ p+A\rightarrow C_3^*+2p; & C_3^*\rightarrow B_2+\gamma \\ p+A\rightarrow C_4^*+2n; & C_4^*\rightarrow B_3+\gamma \\ p+A\rightarrow C_5^*+p+n; & C_5^*\rightarrow B_1+\gamma \end{array}$$

TABLE I. Calculated distribution of various knock-out processes, for 100 incident protons.

Particles ejected	No. of cases
p	11
n	12
$2p$	8
$2n$	5
pn	25

where A is the target nucleus, C^* is the excited residual nucleus, and B is the product nucleus. The contribution from deuteron pick-up is not included, although experiments by Hadley and York[3] indicate that it may be appreciable.

The probabilities of the various initial knock-out processes were calculated on the basis of the model developed by Goldberger.[2] The calculations were performed for $A=64$, $Z=32$, and $R=(1.4\times 10^{-13})A^{\frac{1}{3}}$ cm. The maximum Fermi energy is 24 Mev. If an average binding energy of 8 Mev is assumed, the total well depth is 32 Mev. For protons there is an additional 7 Mev representing the Coulomb barrier. The mean free path as a function of energy was calculated from experimental $n-p$ and $p-p$ cross sections. The value of the $n-n$ cross section used was that obtained from a $n-d$, $n-p$ subtraction by Dejuren and Knable.[4] The calculations followed the technique described by Goldberger[3] and Bernar-

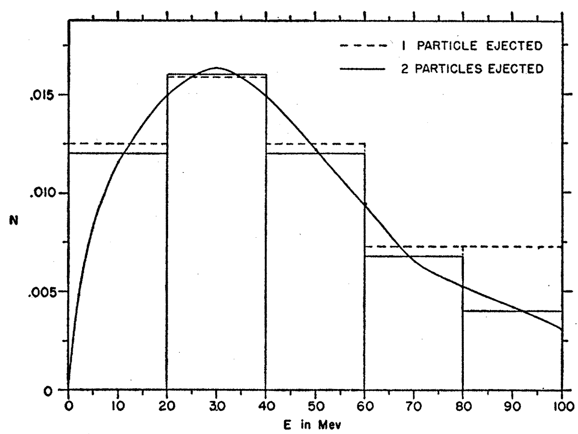

FIG. 1. Distribution of excitation energy in the residual nuclei.

dini *et al.*[5] The results for 100 incident protons applicable to these calculations are shown in Table I and Fig. 1. The secondary evaporation processes were calculated from the statistical theory using constants given by Blatt and Weisskopf.[6]

The experimental cross sections were obtained by a previously described method[7] using enriched isotopes[8] in the case of copper and the natural element in the case of zinc. A comparison of the experimental and calculated cross sections is given in Table II.

There are two factors which may account for the discrepancy between the observed and calculated values. (1) At incident proton energies of 25 Mev, where the statistical model alone should account for all reactions, the observed value is twice the calculated value for the p, pn reactions and about one-half the calculated value for the $p, 2n$ reactions. (2) The same distribution of the

TABLE II. Comparison of calculated and experimental cross sections.

Reaction	σ in millibarns calc.	exptl.
$Cu^{63}(p, pn)Cu^{62}$	23	98
$Cu^{63}(p, 2n)Zn^{62}$	20	7
$Cu^{63}(p, n)Zn^{63}$	6	8
$Cu^{65}(p, pn)Cu^{64}$	34	120
$Zn^{68}(p, 2p)Cu^{67}$	4	14

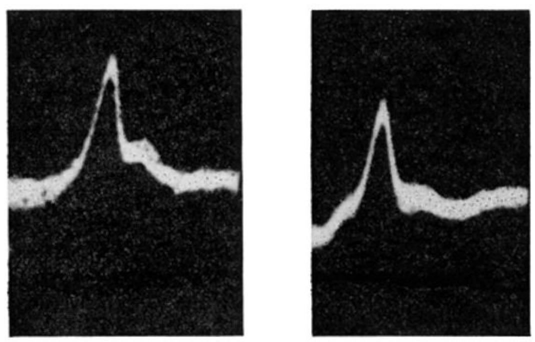

(a) (b)

FIG. 2. Photographs of two sections of spectrum. (a) The line $m=-5/2$ of V^{51} and the satellite $m=-6$ of V^{50}; (b) lines $m=1/2$ of V^{51} and $m=1$ and 2 of V^{50}.